# Calculations of Smith-Purcell radiation generated by electrons of 1–100 MeV

O. Haeberlé, P. Rullhusen, and J.-M. Salomé
*Commission of the European Communities, Joint Research Centre, Institute for Reference Materials and Measurements, Retieseweg, B 2440 Geel, Belgium*

N. Maene
*Vlaamse Instelling voor Technologisch Onderzoek, Boeretang 200, B 2400 Mol, Belgium*
(Received 2 August 1993)

Smith-Purcell radiation is produced when a charged particle moves close to a conducting grating. Recent experiments using electrons of 3.6 MeV have demonstrated the potential use of this effect as a strong tunable radiation source in the infrared spectral range. Large intensities can be expected using high-energy electrons but apparently no detailed calculations have been published until now for this energy domain. We have calculated spectra of Smith-Purcell radiation generated by 1–100-MeV electrons using the integral method, which is of general validity for any type of grating profile, and using the modal expansion method and the improved point-matching method for lamellar and sinusoidal gratings, respectively. The calculations are restricted to perfectly conducting surfaces and to electron trajectories perpendicular to the grating rulings. Some problems related to an extension of the model to include finite electrical conductivity (as needed for calculations of Smith-Purcell radiation in the uv and x-ray spectral range) and for arbitrary tilting angles of the electron beam with respect to the grating rulings are discussed.

PACS number(s): 41.60.−m, 42.25.Fx, 42.79.Dj

## I. INTRODUCTION

In the submillimeter range of the electromagnetic spectrum only a few intense and tunable practical sources are available. Recently, Doucas *et al.* [1] have demonstrated the production of Smith-Purcell (SP) radiation at wavelengths of 0.35–1.86 mm using 3.6-MeV electrons. The intensity observed in this experiment attracted considerable interest in recent literature [2,3] and the SP effect was discussed as a possible tunable source of intense coherent radiation.

In 1942 Frank [4] predicted that a fast electron passing close to a diffractive structure would emit polarized light. The first experimental confirmation was obtained in 1953 by Smith and Purcell [5]. Since then, several studies have been carried out exploring this phenomenon in view of possible applications as a tunable electromagnetic source [6], for particle acceleration [7], or in a free-electron laser [8–11].

In 1960 Toraldo di Francia [12] established the analogy between the Cherenkov and the SP effect. In this approach, the electric field of the moving electron is described by a set of evanescent plane waves and the refraction (Cherenkov effect) or the diffraction (SP) of these waves produces the outgoing light. However, the general problem of electromagnetic-wave diffraction by a periodic surface was not solved at this time, except for some particular structures [13]. Calculations of the SP effect were generally carried out using an approximation based on the Rayleigh hypothesis for shallow gratings [14]. A rigorous solution for arbitrary grating profiles was given by Petit and Maystre [15] and by van den Berg [16], who later on applied this theory to the special case of the SP effect where the incident waves are evanescent [17]. Gover, Dvorkis, and Elisha [18] made a comparison of different models of the SP effect and concluded that the van den Berg model fits best with the experimental data.

To our knowledge up to now in most experiments on the SP effect [5,6,8,11,14,19] only moderately relativistic electrons with energies in the range of some hundred keV have been used. The recent experiment of Doucas *et al.* [1] at 3.6 MeV was the first evidence for the feasibility of using high-energy electrons to produce SP radiation. From these experiments it appears that a strong increase in power of SP radiation can be expected when using higher-energy electron beams.

The purpose of this article is to present theoretical predictions of SP radiation generated by relativistic electrons with energies up to 100 MeV. The calculations are based on the theory developed by Toraldo di Francia [12]. In this approach the Coulomb field of the electron is represented by the superposition of evanescent waves, some of which are diffracted from the grating as propagating waves. We use the integral method, which has the most general validity. For two particular cases we present other approaches which have the advantage of greater ease in calculation. The power radiated in a certain direction of observation is related to the so-called radiation factors, which are analogous to the reflection coefficients in the "classical" diffraction problem of light and are calculated from the reflected-field Fourier transforms.

## II. THEORY

In the following, we adopt with some minor modifications the description of the problem and the no-

 

tation proposed by van den Berg [17], to which the reader is referred for more details. Figure 1 gives a schematical description of the relevant geometrical quantities. The electron moves in vacuum parallel to the surface of a grating with a constant velocity $v_0\mathbf{i}_x$ along the trajectory $y=0$ and $z=z_0=\text{const}$. $\mathbf{i}_x,\mathbf{i}_y,\mathbf{i}_z$ are unit vectors in the $x,y,z$ directions, respectively. The top of the grating is in the $(x,y)$ plane and the grating profile is described by a periodic function $z=f(x)=f(x+D)$ with the direction of the rulings parallel to the $y$ axis. The grating surface is assumed to be electrically perfect conducting. By convention, the vector $\mathbf{n}$ normal to the surface is pointing inside the grating.

The field vectors $\mathbf{E}^i=\mathbf{E}^i(x,y,z,t)$ and $\mathbf{H}^i=\mathbf{H}^i(x,y,z,t)$ of the Coulomb field of the electron are expanded in terms of Fourier integrals:

$$\mathbf{E}^i(x,y,z,t)=(2\pi^2)^{-1}\mathrm{Re}\left[\int_0^\infty d\omega\int_{-\infty}^{\infty}\mathcal{E}^i(x,z;\beta,\omega)\times\exp(i\beta y-i\omega t)d\beta\right], \tag{2.1}$$

$$\mathbf{H}^i(x,y,z,t)=(2\pi^2)^{-1}\mathrm{Re}\left[\int_0^\infty d\omega\int_{-\infty}^{\infty}\mathcal{H}^i(x,z;\beta,\omega)\times\exp(i\beta y-i\omega t)d\beta\right]. \tag{2.2}$$

The $x$ and $z$ components of the Fourier transforms $\mathcal{E}^i,\mathcal{H}^i$ can be expressed as functions of the $y$ components $E_y^i$ and $H_y^i$, which satisfy the two-dimensional Helmholtz equations

$$\partial_x^2E_y^i+\partial_z^2E_y^i+(k_0^2-\beta^2)E_y^i=(\mu_0/\varepsilon_0)^{1/2}(\beta/k_0)\partial_xJ_x\ , \tag{2.3}$$

$$\partial_x^2H_y^i+\partial_z^2H_y^i+(k_0^2-\beta^2)H_y^i=-\partial_zJ_x\ , \tag{2.4}$$

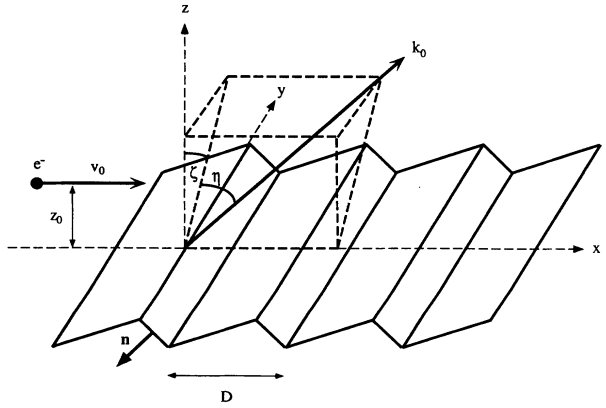


FIG. 1. Schematical layout of the geometry. The electron moves with constant speed $v_0$ at a distance $z_0$ parallel to a perfectly conducting grating and perpendicular to the rulings.

with $\mathcal{J}(x,z;\beta,\omega)=q\exp(i\alpha_0x)\delta(z-z_0)\mathbf{i}_x$, $\alpha_0=\omega/v_0=k_0c_0/v_0$, $q$ is the electron charge, and $c_0$ is the vacuum speed of light. The solutions are given as

$$E_y^i(x,z;\beta,\omega)=\frac{q}{2}(\mu_0/\varepsilon_0)^{1/2}(\beta/k_0)(\alpha_0/\gamma_0)\times\exp(i\alpha_0x+i\gamma_0|z-z_0|)\ , \tag{2.5}$$

$$H_y^i(x,z;\beta,\omega)=-\frac{q}{2}\mathrm{sgn}(z-z_0)\exp(i\alpha_0x+i\gamma_0|z-z_0|)\ , \tag{2.6}$$

in which $\gamma_0=i(\alpha_0^2+\beta^2-k_0^2)^{1/2}$ with $(\alpha_0^2+\beta^2-k_0^2)^{1/2}\geq 0$. Since $v_0<c_0$ we have $\alpha_0>k_0$ and $\gamma_0$ is always imaginary and nonzero. This means that the Coulomb field of the electron is represented by a set of evanescent plane waves exponentially decaying in the direction away from the electron trajectory. In the absence of any perturbing device the free electron moving in empty space does not radiate. But if the electron moves close to a grating these evanescent waves are diffracted by the grating and some of them give rise to propagating reflected plane waves. Therefore the calculation of the SP radiation is reduced to the grating diffraction problem and may be solved by the same techniques.

The reflected field is given by $\mathbf{E}^r=\mathbf{E}-\mathbf{E}^i$ and $\mathbf{H}^r=\mathbf{H}-\mathbf{H}^i$, with $\mathbf{E}=\mathbf{E}(x,y,z,t)$ and $\mathbf{H}=\mathbf{H}(x,y,z,t)$ being the total field above the grating. These reflected fields are also expanded as Fourier integrals in which the Fourier transforms $\mathcal{E}^r,\mathcal{H}^r$ satisfy the source-free Maxwell equations

$$(\nabla+i\beta\mathbf{i}_y)\times\mathcal{E}^r-i\omega\mu_0\mathcal{H}^r=0\ , \tag{2.7}$$

$$(\nabla+i\beta\mathbf{i}_y)\times\mathcal{H}^r+i\omega\varepsilon_0\mathcal{E}^r=0\ , \tag{2.8}$$

and a boundary condition at the surface. For a perfectly conducting surface this boundary condition is

$$\mathbf{n}\times(\mathcal{E}^i+\mathcal{E}^r)=0\ , \tag{2.9}$$

in which $\mathbf{n}$ is the unit vector normal to the surface. For this case it can be shown [16] that the three-dimensional vectorial problem can be separated into two scalar problems of two dimensions called the two fundamental cases of polarization, viz., the $E$ polarization and the $H$ polarization. For the $E$-polarization case, where $E_y\neq 0$ and $H_y=0$, the component $E_y^r=E_y-E_y^i$ satisfies the Helmholtz equation

$$\partial_x^2E_y^r+\partial_z^2E_y^r+(k_0^2-\beta^2)E_y^r=0\ , \tag{2.10}$$

with the boundary condition $E_y=0$ on the surface of the grating. For the $H$-polarization case, where $H_y\neq 0$ and $E_y=0$, the Fourier component $H_y^r=H_y-H_y^i$ satisfies the Helmholtz equation

$$\partial_x^2H_y^r+\partial_z^2H_y^r+(k_0^2-\beta^2)H_y^r=0\ , \tag{2.11}$$

with the boundary condition $\mathbf{n}\cdot\nabla H_y=0$ on the surface. The reflected field above the grating $(z>0)$ can be represented by a Rayleigh expansion which describes the field in terms of propagating and evanescent waves:

$$E_y^r(x,z;\beta,\omega)=\sum_{n=-\infty}^{\infty} E_{y,n}^r(\beta,\omega)\exp(i\alpha_n x+i\gamma_n z)\ , \tag{2.12}$$

$$H_y^r(x,z;\beta,\omega)=\sum_{n=-\infty}^{\infty} H_{y,n}^r(\beta,\omega)\exp(i\alpha_n x+i\gamma_n z)\ , \tag{2.13}$$

in which $\alpha_n=\alpha_0+2\pi n/D$ and $\gamma_n=(k_0^2-\beta^2-\alpha_n^2)^{1/2}$ with $\mathrm{Re}(\gamma_n)\geq 0$ and $\mathrm{Im}(\gamma_n)\geq 0$. The SP radiation is the sum of all emerging propagating waves, i.e., those waves for which $\mathrm{Im}(\gamma_n)=0$. Therefore $\alpha_n^2+\beta^2\leq k_0^2$ and only negative orders $n$ can contribute. The angles of emergence $\eta_n$ and $\zeta_n$ satisfy the relations [17]

$$\alpha_n=k_0\sin(\eta_n)\ , \tag{2.14}$$

$$\beta=k_0\cos(\eta_n)\sin(\zeta_n)\ , \tag{2.15}$$

$$\gamma_n=k_0\cos(\eta_n)\cos(\zeta_n)\ . \tag{2.16}$$

From (2.14) the following relation is obtained for the wavelength $\lambda_0=2\pi/k_0$:

$$-n\lambda_0=D[c_0/v_0-\sin(\eta_n)]\ . \tag{2.17}$$

According to (2.17) photons of fixed wavelength $\lambda_0$ are emitted at different angles of observation $\eta_n$ in different emission orders $n$. Since $|\sin(\eta_n)|\leq 1$, the number of angles $\eta_n$ at which this wavelength $\lambda_0$ is emitted is given by

$$|n_{\max}|=[c_0/v_0+1]D/\lambda_0\ . \tag{2.18}$$

In order to find the intensity of one of these propagating waves the coefficients $E_{y,n}^r$ and $H_{y,n}^r$ in the Rayleigh expansions (2.12) and (2.13) have to be calculated. This problem, referred to as the *grating problem,* has been treated in detail in literature [20]. In the forward direction and using high-energy electrons, $D/\lambda_0$ becomes very large and the computational effort becomes appreciable. We have applied some of the now available methods to calculate the radiation produced by a relativistic electron beam and give a brief description of these methods in the following section.

## III. SOLUTION OF THE GRATING PROBLEM

### A. The Rayleigh method

A simple method to solve the grating problem is to assume that the Rayleigh expansion (2.12) and (2.13) is valid also inside the grooves of the grating and to apply the boundary conditions at the surface of the grating. It was used [21] in calculations of SP radiation for shallow gratings with triangular profile. However, it has been shown [20,22] that this method is not generally valid, e.g., for deep sinusoidal gratings, and we did not use it.

### B. The integral method

The integral method [15,16] was used by van den Berg [17] to give the first complete treatment of the SP effect. The method makes use of the two-dimensional form of the Green's theorem to obtain the coefficients $E_{y,n}^r$ and $H_{y,n}^r$ as functions of the total field at the surface of the grating:

$$E_{y,n}^r=\frac{i}{2\gamma_n D}\int_L(\mathbf{n}\cdot\nabla E_y)\exp(-i\alpha_n x-i\gamma_n z)ds\ , \tag{3.1}$$

$$H_{y,n}^r=-\frac{i}{2\gamma_n D}\int_L H_y(\mathbf{n}\cdot\nabla)\exp(-i\alpha_n x-i\gamma_n z)ds\ , \tag{3.2}$$

in which the path of integration $L$ is at the grating surface along one period of the grating at constant $y$.

Applying Green's theorem, one arrives [17] at a set of integral equations of either first or second kind, in which the equations of second kind for $\mathbf{n}\cdot\nabla E_{y,n}^r$ and $H_{y,n}^r$ have the same structure. The numerical solution of integral equations of the second kind is generally easier than for integral equations of the first kind because of singularities in the kernels of the integrals. Following van den Berg [17] we use the following integral equations of second kind, i.e., for the two fundamental cases of polarization:

$$\tfrac{1}{2}\mathbf{n}_p\cdot\nabla_p E_y(x_p,z_p)+P\int_L(\mathbf{n}\cdot\nabla E_y)(-\mathbf{n}_p\cdot\nabla_p G)ds=\mathbf{n}_p\cdot\nabla_p E_y^i(x_p,z_p)\ , \tag{3.3}$$

$$\tfrac{1}{2}H_y(x_p,z_p)+P\int_L H_y(\mathbf{n}\cdot\nabla G)ds=H_y^i(x_p,z_p)\ , \tag{3.4}$$

where the point $(x_p,y_p)$ is on $L$ and $P$ denotes the Cauchy principal value of the integral. Green's function $G$ is given by

$$G(x,z;x_p,z_p)=\sum_{n=-\infty}^{+\infty}(i/2\gamma_n D)\exp\{i\alpha_n(x_p-x)+i\gamma_n|z_p-z|\}\ . \tag{3.5}$$

The set of integral equations (3.3) and (3.4) can be solved using a discrete Fourier transformation and truncating the infinite system of equations. This method, however, is recommended only for cases where the coefficients of the system can be obtained analytically, e.g., for triangular and trapezoidal grating profiles [16,20]. A more general method to solve the grating problem consists in a discretization of the unknown functions $\mathbf{n}\cdot\nabla E_y$ and $H_y$ at $N$ points on the surface. This leads to a matrix equation of order $N$. Since this method can be used for any kind of grating profile we have chosen to use it in our calculations. For details of this method the reader is referred to the paper of van den Berg [16] and to the book of Petit [20].

### C. The improved point-matching method

Exact results can be obtained using a variational method [23], with moderate computational effort for shallow gratings. This method is called the improved point-matching method (IPMM). We use a procedure in analogy to the method used by Ikuno and Yasuura [24] to calculate the diffraction of light. In this approach $E_y^r$ and $H_y^r$ are approximated by truncated Rayleigh expansions

and the coefficients of these expansions are found minimizing the following quantities $I_E$ and $I_H$ for the two fundamental cases of polarization:

$$I_E=\int_L |E_y^i+E_y^r|^2 ds \ , \tag{3.6}$$

$$I_H=\int_L |\mathbf{n}\cdot\nabla(H_y^i+H_y^r)|^2 ds \ . \tag{3.7}$$

The truncated Rayleigh expansions used for $E_y^r$ and $H_y^r$ are

$$E_y^r(x,z;\beta,\omega)=\sum_{n=-N}^{+N} E_{y,n}^r(N;\beta,\omega)\exp(i\alpha_n x+i\gamma_n z) \tag{3.8}$$

and

$$H_y^r(x,z;\beta,\omega)=\sum_{n=-N}^{+N} H_{y,n}^r(N;\beta,\omega)\exp(i\alpha_n x+i\gamma_n z) \ . \tag{3.9}$$

It has been proven [24–26] that both quantities $I_E$ and $I_H$ vanish for $N\to\infty$ and the set of coefficients $E_{y,n}^r(N;\beta,\omega)$ and $H_{y,n}^r(N;\beta,\omega)$ in (3.8) and (3.9) converges to the Rayleigh coefficients $E_{y,n}^r$ and $H_{y,n}^r$ in (2.12) and (2.13). Minimizing $I_E$ and $I_H$, we obtain two systems of linear equations which can be expressed in the form of matrix equations $M\times E=V$ and $M\times H=V$. For the $E$ polarization, one obtains [24] the following elements of the matrix $M$ and of the vector $V$:

$$M_{p,n}=\int_L \exp\left[i(n-p)\frac{2\pi}{D}x+i(\gamma_n-\gamma_p^*)f(x)\right]ds \ , \tag{3.10}$$

$$V_p=\int_L \exp\left[i(-p)\frac{2\pi}{D}x+i(-\gamma_0-\gamma_p^*)f(x)\right]ds \ , \tag{3.11}$$

and for the $H$ polarization

$$M_{p,n}=\int_L [i\alpha_n f'(x)-i\gamma_n][i\alpha_p f'(x)-i\gamma_p]^* \times[1+f'(x)^2]^{-1} \times\exp\left[i(n-p)\frac{2p}{D}x+i(\gamma_n-\gamma_p^*)f(x)\right]ds \ , \tag{3.12}$$

$$V_p=\int_L [i\alpha_0 f'(x)+i\gamma_0][i\alpha_p f'(x)-i\gamma_p]^*[1+f'(x)^2]^{-1} \times\exp\left[i(-p)\frac{2p}{D}x+i(-\gamma_0-\gamma_p^*)f(x)\right]ds \ . \tag{3.13}$$

The size of the matrix systems is increased until convergence to the desired level of accuracy is obtained. For deep gratings the computation time increases drastically and the integral method becomes preferable [26]. We have used the IPMM for moderately deep sinusoidal gratings with a height $h<0.25D$ making the approximation $|f'(x)|\ll 1$ and $ds=\sqrt{1+f'(x)^2}dx\approx dx$. Then, $M_{p,n}$ and $V_p$ can be calculated analytically in terms of Bessel functions. We found agreement better than 10% with the results obtained using the integral method.

### D. Modal expansion method

In the $(x,z)$ plane, i.e., for $\zeta=0°$, the SP effect is reduced to the study of the $H$-polarization diffraction because $\zeta=0$ implies $\beta=0$, for which the $E$-polarized contribution of the incoming waves vanishes. In this special case the formalism is very similar to the one applied in calculations of SP radiation from a line charge extended in $y$ direction and moving in $x$ direction parallel to a grating. Such a theory was derived by van den Berg [27] for gratings of rectangular profile (lamellar gratings) using the treatment of Deryugin [28]. Figure 2 shows schematically the relevant parameters. Again, the electric and magnetic fields are represented by Fourier integrals, which are given in the following form because of the two-dimensional nature of the problem:

$$\mathbf{E}(x,z,t)=\pi^{-1}\mathrm{Re}\left[\int_0^\infty \mathcal{E}(x,z;\omega)\exp(-i\omega t)d\omega\right] , \tag{3.14}$$

$$\mathbf{H}(x,z,t)=\pi^{-1}\mathrm{Re}\left[\int_0^\infty \mathcal{H}(x,z;\omega)\exp(-i\omega t)d\omega\right] . \tag{3.15}$$

In this case, $\mathcal{H}$ has only a $y$ component

$$\mathcal{H}=U\mathbf{i}_y \tag{3.16}$$

and

$$\mathcal{E}=(i\omega\varepsilon_0)^{-1}[J_x\mathbf{i}_x+\partial_z U\mathbf{i}_x-\partial_x U\mathbf{i}_z] \ , \tag{3.17}$$

in which $J_x$ represents the Fourier transform of the current density $qv_0\delta(x-v_0t,z-z_0)$. $U(x,z;\omega)$ satisfies the two-dimensional Helmholtz equation and the boundary condition $\mathbf{n}\cdot\nabla U=0$ at the grating surface. Above the grating $(z>0)$ $U(x,z;\omega)$ is given [27] by

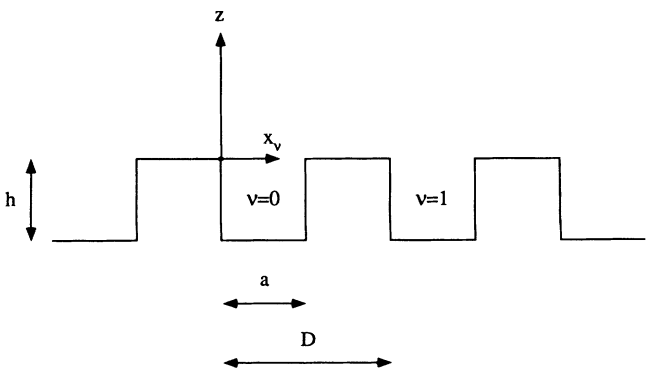


FIG. 2. Geometry of a lamellar grating profile.

$$U(x,z;\omega)=-\frac{q}{2}\mathrm{sgn}(z-z_0)\exp(i\alpha_0 x+i\gamma_0|z-z_0|)$$
$$+\sum_{n=-\infty}^{\infty}U_n^r(\omega)\exp(i\alpha_n x+i\gamma_n z)\ . \quad (3.18)$$

Inside the grooves ($z<0$) $U(x,z;\omega)$ is obtained from the known solutions of waveguide modes

$$U(x_\nu,z;\omega)=\exp(i\alpha_0\nu D)\times\sum_{m=0}^{\infty}A_m\cos(m\pi x_\nu/a)\times[\exp(-i\kappa_m z)+\Gamma_m\exp(+i\kappa_m z)]\ , \quad (3.19)$$

with $0<x_\nu<a$, $-h<z<0$, $\kappa_m=\{k_0^2-(m\pi/a)^2\}^{1/2}$, $\Gamma_m=\exp(2i\kappa_m h)$, and $x_\nu$ denotes the local $x$ coordinate in the $\nu$th groove, i.e., $x=\nu D+x_\nu$. Using the boundary conditions for the field at the open end of the grooves ($0<x_\nu<a$) and on the ridges ($a<x_\nu<D$) the following system of equations is obtained [27]:

$$\sum_{n=-\infty}^{\infty}(\gamma_n D\delta_{k,n}-V_{k,n})U_n^r=C_k\quad(k=0,\pm1,\pm2,\ldots) \quad (3.20)$$

in which

$$C_k=\frac{q}{2}\exp(i\gamma_0 z_0)\left[\gamma_0 D\delta_{k,0}+a\sum_{m=0}^{\infty}\varepsilon_m\kappa_m\frac{\Gamma_m-1}{\Gamma_m+1}\Psi_{m,k}\Psi^*_{m,0}\right]\ , \quad (3.21)$$

$$V_{k,n}=a\sum_{m=0}^{\infty}\varepsilon_m\kappa_m\frac{\Gamma_m-1}{\Gamma_m+1}\Psi_{m,k}\Psi^*_{m,n}\ , \quad (3.22)$$

$$\Psi_{m,n}=a^{-1}\int_0^a\cos(m\pi x/a)\exp(-i\alpha_n x)dx\ , \quad (3.23)$$

and $\varepsilon_k=2-\delta_{k,0}$. In order to find the unknown factors $U_n^r$ this infinite system of equations is truncated and the order of truncation is increased until convergence is achieved.

One advantage of the modal expansion method (MEM) is the speed of computation. The coefficients of the matrix system can be calculated analytically whereas for the integral method this has to be done numerically. Another advantage is that the inversion of the matrix system gives directly the solution for all different modes whereas for the integral method first the fields on the surface have to be calculated and then one integral for each diffracted order has to be calculated numerically. Furthermore, the MEM automatically takes care of the singularities at the edges of the rectangular profile, which require a special treatment when using an integral formalism. We compared the results to calculations using the integral method for lamellar gratings, approximating the rectangular grating profile by a differentiable function $z=f(x)$. We found good agreement of the results but the computational time became long. Therefore, for lamellar gratings we present only the results obtained using the MEM. A similar method can be used for gratings of symmetric triangular profile [20,29], but in this case the integral method is also well suited and is recommended because it is valid for all kinds of triangular gratings, as explained in Sec. II.

## IV. RESULTS

The energy loss due to emission of SP radiation of a single electron of charge $q=-e$ when traversing one period of the grating at a distance $z_0$ above the surface is given [18] by

$$W=\frac{e^2}{D\varepsilon_0}\sum_n\int_{-\pi/2}^{+\pi/2}\int_{-\pi/2}^{+\pi/2}\frac{\cos^2\eta\cos^2\zeta}{(\beta^{-1}-\sin\eta)^3}|R_n(\beta,\eta,\zeta)|^2\times\exp\left[-\frac{z_0}{h_{\mathrm{int},n}(\eta,\zeta)}\right]\times\cos\eta\,d\eta\,d\zeta \quad (4.1)$$

with

$$h_{\mathrm{int},n}=\frac{D(\beta^{-1}-\sin\eta)}{4\pi|n|(\beta^{-2}-1+\cos^2\eta\sin^2\zeta)^{1/2}}=\frac{\lambda_n}{4\pi(\beta^{-2}-1+\cos^2\eta\sin^2\zeta)^{1/2}}\ , \quad (4.2)$$

which gives

$$h_{\mathrm{int},n}=\frac{\lambda_n}{4\pi}\beta\gamma \quad (4.3)$$

in the plane $\zeta=0°$. In (4.2) and (4.3) we have introduced the reduced speed $\beta=v_0/c_0$ and the Lorentz factor $\gamma=(1-\beta^2)^{-1/2}$. The summation is to be taken over all propagative orders $n$. The parameter $h_{\mathrm{int},n}$ can be considered as an effective interaction range analogue to the "formation zone" found in other types of radiation, e.g., transition radiation and the Cherenkov effect. The so-called radiation factors $|R_n(\beta,\eta,\zeta)|^2$ correspond to the classical reflection coefficients of a grating and are given by [17]

$$|R_n(\beta,\eta,\zeta)|^2=\frac{4}{e^2}\exp(2|\gamma_0|z_0)\left\{\frac{\varepsilon_0}{\mu_0}|E^r_{y,n}|^2+|H^r_{y,n}|^2\right\}\times(1-\cos^2\eta\sin^2\zeta)^{-1}\ . \quad (4.4)$$

The term $\exp(2|\gamma_0|z_0)$ in (4.4) is introduced in order to compensate for the $z_0$ dependence of $E^r_{y,n}$ and $H^r_{y,n}$. With this definition, the radiation factors do not depend on the distance $z_0$ of the electron trajectory to the grating surface and the total power of SP radiation emitted by an electron beam is obtained integrating (4.1) analytically over $y$ and $z_0$, i.e., over the beam profile. Assuming an electron beam of width $b$ smaller than the width $B$ of the grating and of height $h\gg h_{\mathrm{int}}$, with a constant current density $J_0$ and passing over a grating of length $L$ and period $D$, the power emitted in order $n$ by the beam per unit solid angle in direction $(\eta,\zeta)$ is given [18] by

$$dP/d\Omega = F \times G(\beta,\eta,\zeta)|R_n(\beta,\eta,\zeta)|^2$$
$$= \frac{eJ_0bL}{4\pi\varepsilon_0 D|n|} \times \frac{\cos^2\eta\cos^2\zeta}{(\beta^{-1}-\sin\eta)^2(\beta^{-2}-1+\cos^2\eta\sin^2\zeta)^{1/2}} \times |R_n(\beta,\eta,\zeta)|^2 . \quad (4.5)$$

The first factor $F$ characterizes the experimental setup and includes the current density, the size of the electron beam, the size and the period of the grating, and the order of diffraction that is observed. The second factor $G(\beta,\eta,\zeta)$ is a function of the energy of the electron and the angles of observation $\eta$ and $\zeta$. Figure 3 shows the $\eta$ dependence of this factor $G(\beta,\eta,\zeta)$ at electron energies of 100 keV and 50 MeV. At 50 MeV $G(\beta,\eta,\zeta)$ strongly increases in the forward direction $\eta \approx 90°$ where short wavelengths are produced and this effect becomes more prominent at higher energies. Figure 4 shows the $\zeta$ dependence of $G(\beta,\eta,\zeta)$ at 100 keV and 50 MeV and for several values of $\eta$. A strong effect of polarization seems to appear when the energy of the incoming electrons increases: the radiation is concentrated in the $(x,z)$ plane where the incoming radiation is $H$ polarized. This effect is more pronounced for observation near $\eta \approx 0°$. Under favorable conditions the strong $\zeta$ dependence of $G(\beta,\eta,\zeta)$ can be used to design a quasimonochromatic and polarized radiation source.

The intensity of the observed SP radiation depends, of course, on the behavior of the radiation factor $|R_n(\beta,\eta,\zeta)|^2$, which strongly depends on the energy of

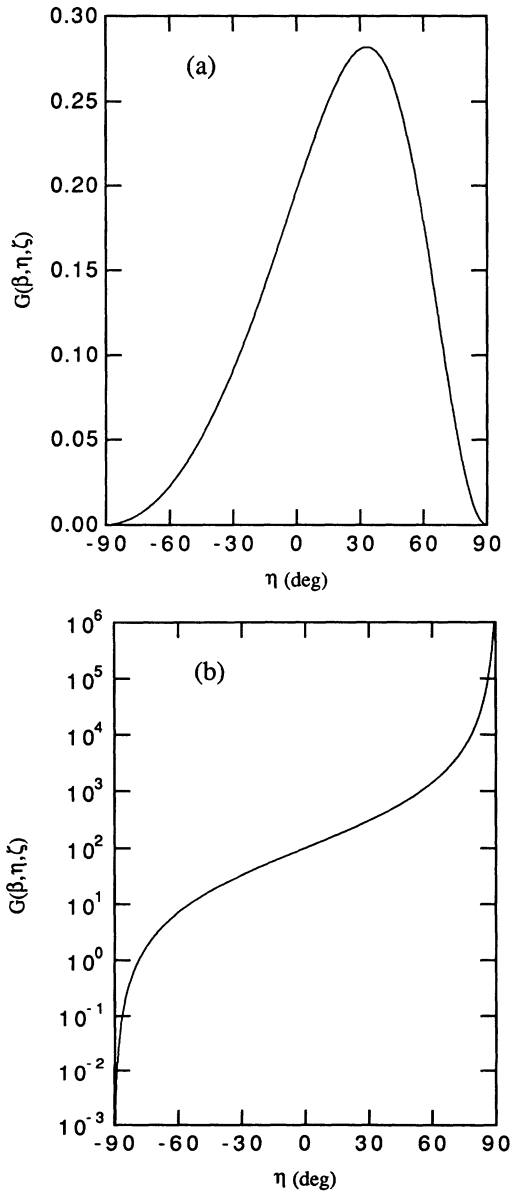


FIG. 3. The $\eta$ dependence of $G(\beta,\eta,\zeta)$ for $\zeta=0°$ and electron energies of (a) 100 keV and (b) 50 MeV.

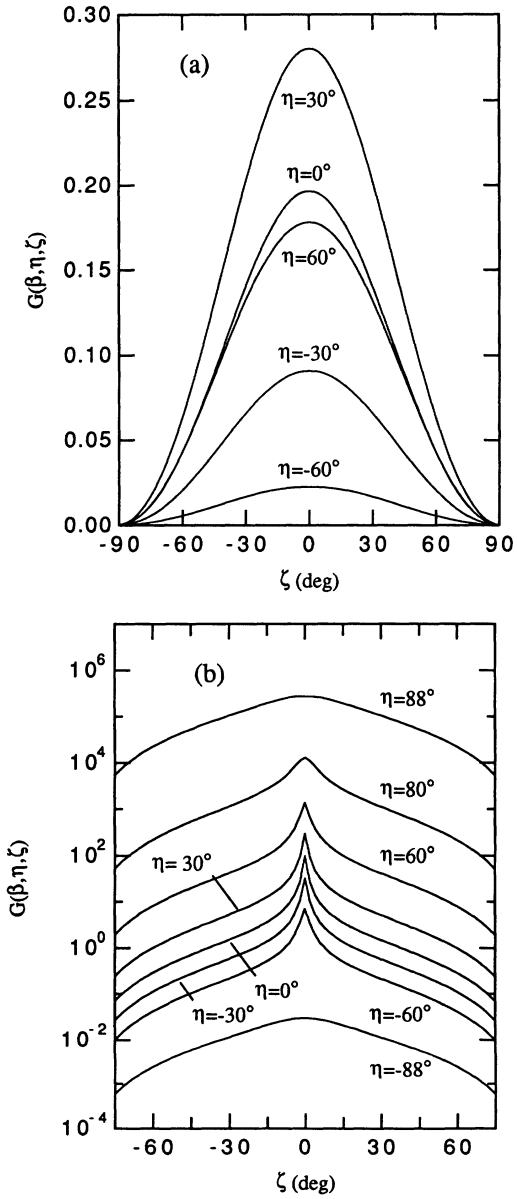


FIG. 4. The $\zeta$ dependence of $G(\beta,\eta,\zeta)$ for several angles $\eta$ and electron energies of (a) 100 keV and (b) 50 MeV.

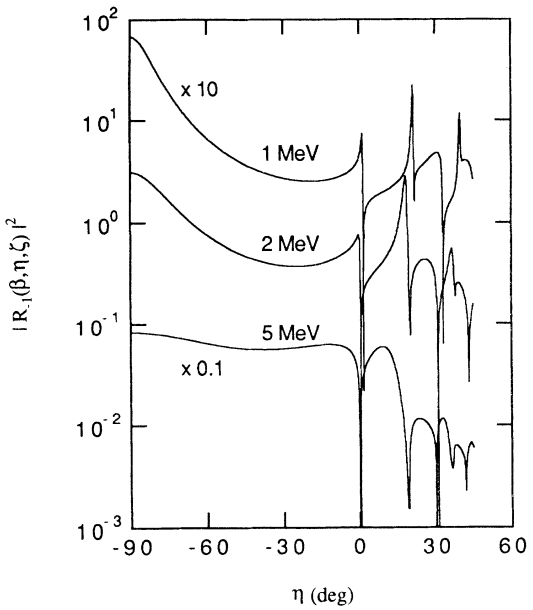


FIG. 5. Radiation factors $|R_{-1}(\beta,\eta,\zeta)|^2$ for a lamellar grating as a function of observation angle $\eta$ for $\zeta=0°$ and for electron energies of 1, 2, and 5 MeV. The grating parameters are $h/D=0.1$ and $a/D=0.5$. The data for 1 and 5 MeV have been multiplied by factors of 10 and 0.1, respectively.

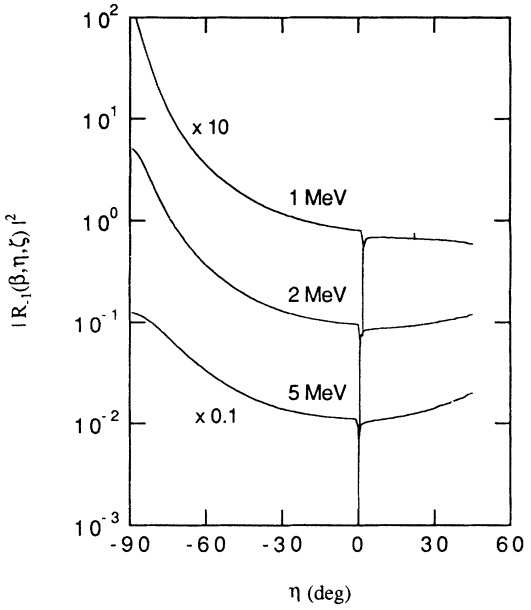


FIG. 7. Radiation factors $|R_{-1}(\beta,\eta,\zeta)|^2$ for a sinusoidal grating with $h/D=0.1$ as a function of observation angle $\eta$ for $\zeta=0°$ and for electron energies of 1, 2, and 5 MeV. The data for 1 and 5 MeV have been multiplied by factors of 10 and 0.1, respectively.

the electron and on the grating profile. It mainly determines the spectra of SP radiation. In Figs. 5–8 we present some results of our calculations of the radiation factor $|R_{-1}(\beta,\eta,\zeta)|^2$. All values have been calculated for the first propagative order $n=-1$ and for an observation angle $\zeta=0°$, for which the intensity is expected to be largest. We have restricted our calculations to observation angles $\eta<45°$ where reliable convergence of the numerical solution of the integral equations was obtained. Two types of gratings have been considered, viz., lamellar and sinusoidal profiles.

The radiation factors for rectangular profiles are functions of the ratios $h/D$ and $a/D$, for which we have chosen $h/D=0.1$ and $a/D=0.5$ in our calculations. As explained above, we used both the MEM and the integral method and found overall good agreement. In Figs. 5 and 6 the $\eta$ dependence of the radiation factors

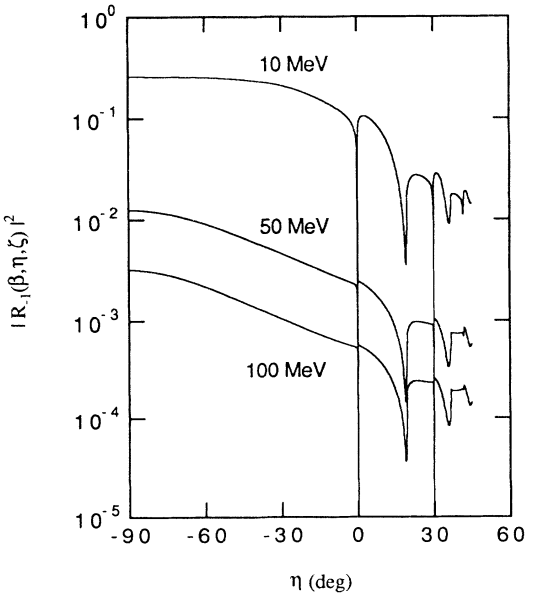


FIG. 6. Same as Fig. 5 but for electron energies of 10, 50, and 100 MeV.

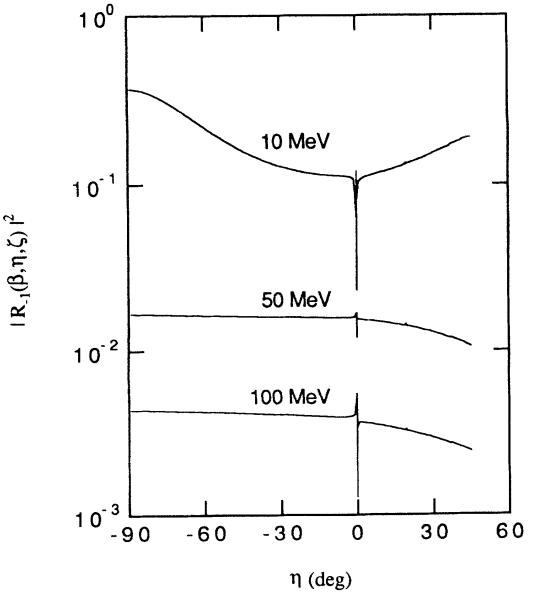


FIG. 8. Same as Fig. 7 but for electron energies of 10, 50, and 100 MeV.

$|R_{-1}(\beta,\eta,\zeta)|^2$ as calculated using the MEM are given for several electron energies between 1 and 100 MeV. Strong variations of the radiation factor can be seen near certain values $\eta=\eta_w$ in the forward direction. These resonances are related to the Wood-Rayleigh anomalies [20,27] where an evanescent reflected wave becomes radiating. The angles where these anomalies appear are given by the condition $\gamma_n=0$, from which one obtains $\sin(\eta_w)=n^{-1}\{(n-1)\beta^{-1}-1\}$ with integer numbers $n$. We performed the calculations on an angular mesh of 0.25° except near these anomalies, where we calculated at angles $\eta_w\pm(10^{-7},10^{-4},10^{-3})$. In most cases a strong decrease of the radiation factor is observed at angles near $\eta_w$, but in certain cases also a strong increase of the radiation factor is observed (see, e.g., in Fig. 5 the sharp peak just before $\eta=20°$ for an electron energy of 2 MeV). At these angles the SP radiation is strongly collimated. It is worthwhile to note that the radiation factors decrease with increasing energy. A more detailed investigation shows that this energy dependence of the radiation factors is moderate for electron energies of 1–5 MeV but very strong at higher energies.

For the sinusoidal grating we have chosen a ratio $h/D=0.1$. For such a shallow grating the radiation factors can be calculated using either the integral method or the IPMM. We have used both methods and obtained good agreement. Figures 7 and 8 show the results obtained by the integral method. The radiation factors de-

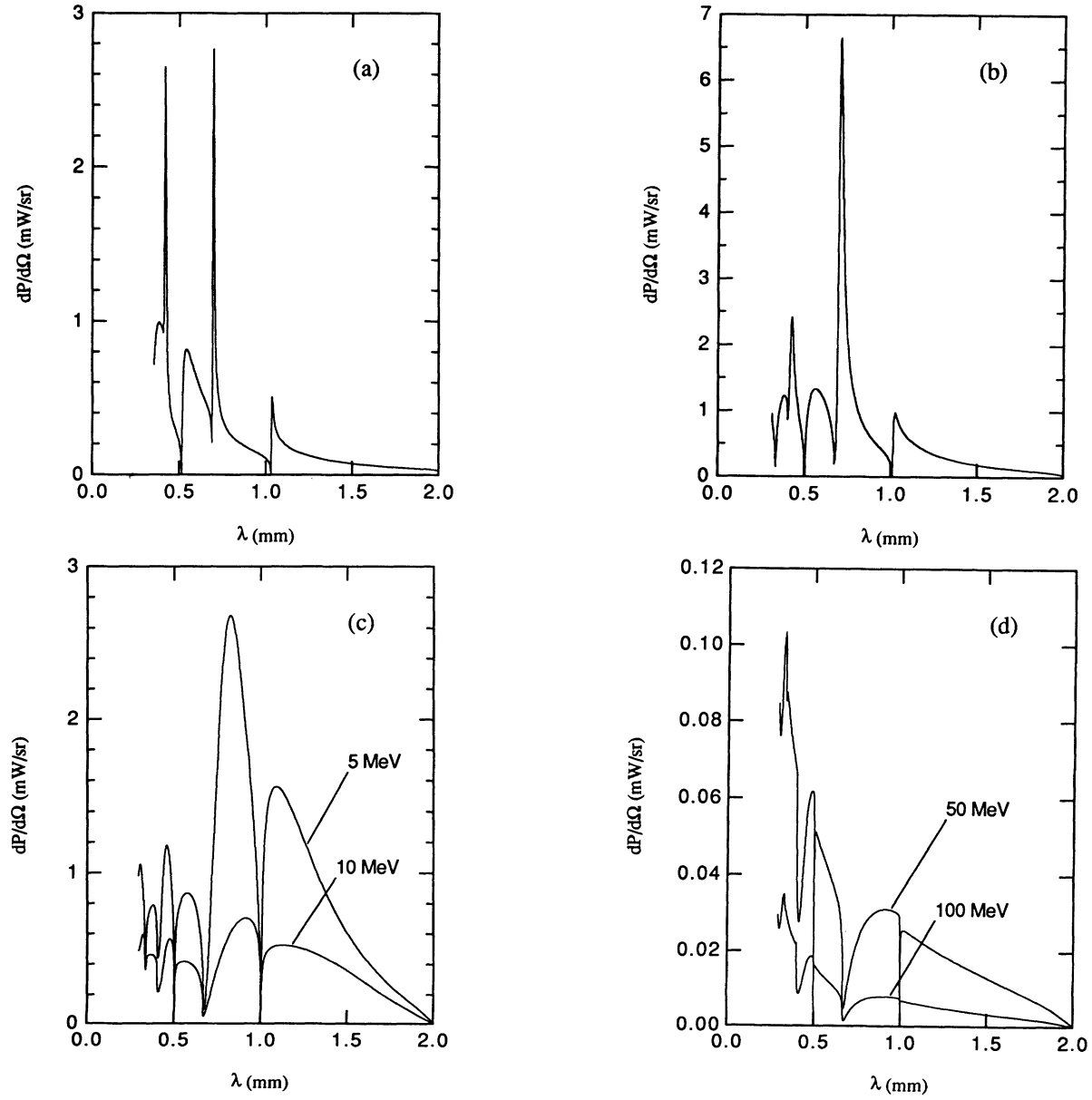


FIG. 9. Spectra of SP radiation in first order at $\zeta=0°$ using a lamellar grating with $B=5$ cm, $L=10$ cm, $D=1$ mm, $h/D=0.1$, and $a/D=0.5$. Gaussian beam profile with $\sigma_y=\sigma_z=1.5$ mm at $z_0=1.5$ mm. Peak current of 10 A. Electron energies of (a) 1 MeV, (b) 2 Mev, (c) 5 and 10 MeV, and (d) 50 and 100 MeV.

crease strongly with increasing energy. Contrary to the results obtained for lamellar gratings, the $\eta$ dependence is rather smooth and fluctuations are restricted to a very narrow angular interval near a Wood-Rayleigh anomaly.

Figures 9–12 show power distributions of SP radiation expressed in mW/sr for some of the gratings and electron energies discussed above. In order to arrive at realistic numbers we did not use Eq. (4.5) but integrated (4.1) over a beam profile represented by a two-dimensional Gaussian distribution. It is assumed that the beam axis is at a distance $z_0$ above the grating, which is shielded against electrons at $z<0$. No angular divergence of the electron beam is considered. In such a situation a similar expression as (4.5) can be used but the factor $F$ has to be replaced by

$$F=\frac{ei_0L}{4\pi\varepsilon_0 D|n|h_{\text{int}}}\operatorname{erf}\left[\frac{B}{\sqrt{8}\sigma_y}\right]\exp\left[\frac{c^2}{4}-s_0\right]\times\left\{1-\operatorname{erf}\left[\frac{c}{2}-\frac{s_0}{c}\right]\right\}, \tag{4.6}$$

in which $i_0=J_0 2\pi\sigma_y\sigma_z$ is the total current, $c=2^{1/2}\sigma_z/h_{\text{int}}$, $s_0=z_0/h_{\text{int}}$, and $b=B/h_{\text{int}}$. In our calculations we used beam parameters achievable at modern linear accelerators, i.e., a peak current $i_0=10$ A and

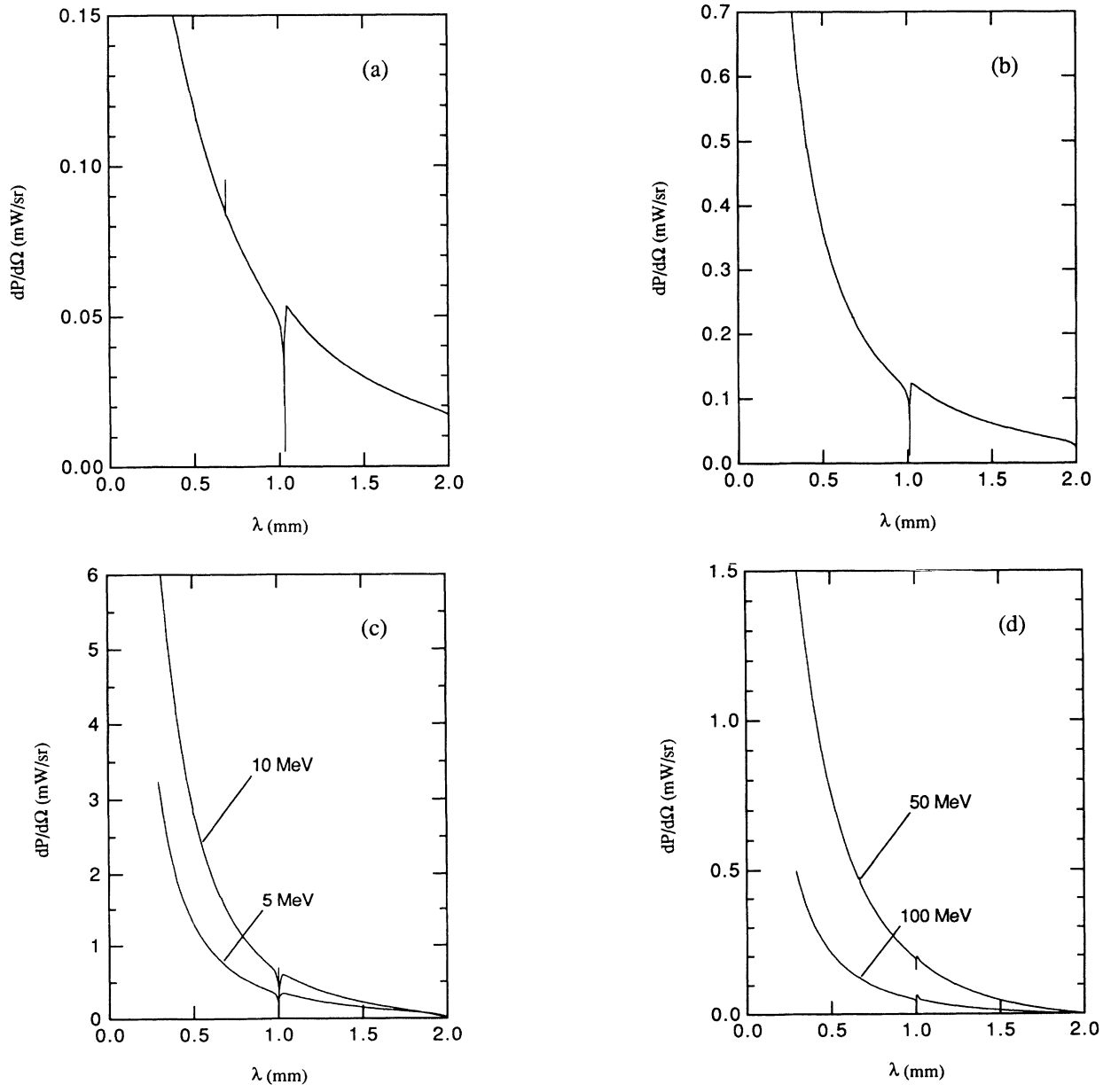


FIG. 10. Spectra of SP radiation in first order at $\zeta=0°$ using a sinusoidal grating with $B=5$ cm, $L=10$ cm, $D=1$ mm, and $h/D=0.1$. Same beam parameters as in Fig. 9. Electron energies of (a) 1 MeV, (b) 2 MeV, (c) 5 and 10 MeV, and (d) 50 and 100 MeV.

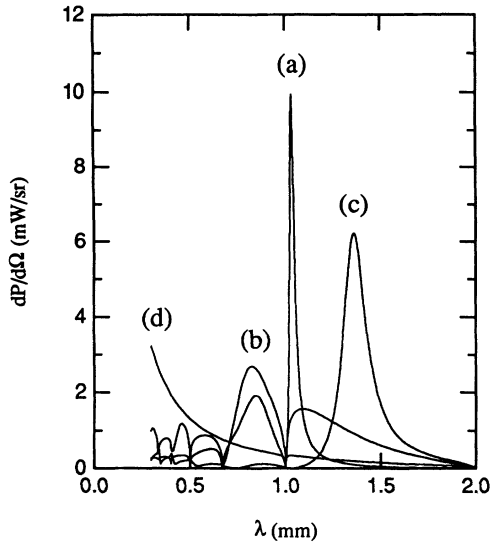


FIG. 11. Comparison of SP spectra in first order at $\zeta=0°$ using 5-MeV electron beams and different gratings with $B=5$ cm, $L=10$ cm, $D=1$ mm: (a) lamellar grating with $h/D=0.1$ and $a/D=0.1$; (b) lamellar grating with $h/D=0.1$ and $a/D=0.5$; (c) lamellar grating with $h/D=0.1$ and $a/D=0.9$; and (d) sinusoidal grating with $h/D=0.1$. Same beam parameters as in Figs. 9 and 10.

$\sigma_y=\sigma_z=1.5$ mm. The beam axis is at $z_0=1.5$ mm, which corresponds to $h_{\text{int}}$ at electron energies of 10 MeV and wavelengths of about 1 mm. The grating dimensions are $B=5$ cm and $L=10$ cm and the grating period is $D=1$ mm. The plane of observation is always at $\zeta=0°$, i.e., perpendicular to the surface of the grating. We present the results as a function of the wavelength using Eq. (2.17).

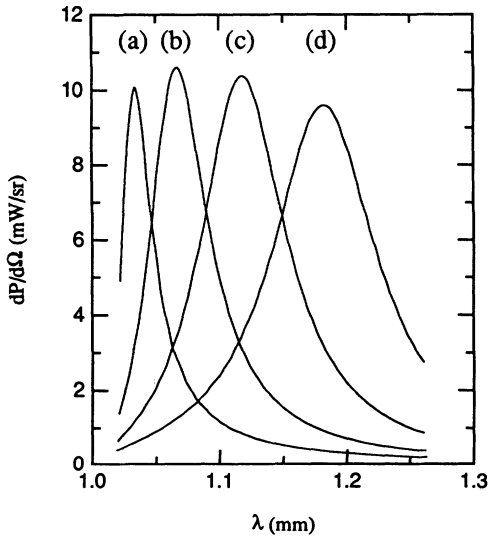


FIG. 12. SP spectra at $\zeta=0°$ using a lamellar grating with $B=5$ cm, $L=10$ cm, $D=1$ mm, $h/D=0.1$, and $a/D=0.1$. Same beam parameters as in Figs. 9–11. Electron energies of (a) 5 MeV, (b) 6 MeV, (c) 7 MeV, and (d) 8 MeV.

We did not try to optimize the beam and grating parameters to find a maximum radiative power. The results can easily be adapted to different experimental configurations using Eqs. (4.5) and (4.6) as long as the same types of gratings and the same electron energies are used. Obviously a beam profile of small height elongated in $y$ direction would be more advantageous. Since the radiation factors do not depend explicitly on the grating period $D$ but only on the ratios $h/D$ and $a/D$ the results can also be used for different grating periods as long as these ratios remain the same. The wavelength range changes, of course, according to (2.17).

It is worthwhile to note that (4.6) takes into consideration a finite beam size of Gaussian shape but assumes a nondivergent electron beam ($|\Theta| \leq h_{\text{int}}/L$ is probably a good approximation). It would be straightforward to adapt (4.6) to electron beams of finite divergence integrating (4.1) over the beam profile, which varies as a function of $x$. This approach, however, would assume an electron trajectory considered as stepwise parallel to the grating surface along one period $D$ and we did not use it. The problem of oblique incidence of the electrons will be discussed below.

## V. DISCUSSION

### A. Numerical difficulties

The application of the different methods outlined above to the calculation of SP radiation implies some peculiar numerical difficulties not seen in the "classical" diffraction theory of gratings. (i) The amplitude of the incident field can vary rapidly in the grooves of the grating, whereas it is constant when the grating is illuminated with a classical source. Therefore, when a discretization procedure is used in the integral method as explained in Sec. III C, the number of points used on the surface of the grating has to be chosen carefully. Since the exponential decrease of the incoming wave is related to the quantity $c_0/v_0$, this is more problematic when using low-energy electrons of a few hundred keV. (ii) In classical spectroscopy use can be made of the energy conservation theorem, stating that the diffracted energy must be equal to the known incoming energy. In the case of SP radiation this energy conservation theorem cannot be used. A modified formula was derived by van den Berg [17] relating the amplitudes of the propagative diffracted waves of order $n$ to the amplitude of the zero-order evanescent wave:

$$\sum_n |E^r_{y,n}|^2 \gamma_n = -e(\mu_0/\varepsilon_0)^{1/2}(\beta/k_0)\alpha_0 \times \mathrm{Re}[E^r_{y,0}\exp(i\gamma_0 z_0)] , \tag{5.1}$$

$$\sum_n |H^r_{y,n}|^2 \gamma_n = e\,\mathrm{Re}[H^r_{y,0}\gamma_0\exp(i\gamma_0 z_0)] , \tag{5.2}$$

in which the summation is taken over all propagative orders $n$. As mentioned in the preceding sections, in our algorithm for the integral method we increase the number of points of the surface discretization, the number of terms in the Green's function, and the number of orders

taken in the Rayleigh expansion until convergence is achieved. Then we use relations (5.1) and (5.2) as a check for the validity of the results. Similar checks are used in the MEM and IPMM calculations.

### B. Practical aspects

Spectra of SP radiation in the millimeter wavelength range obtained using lamellar or sinusoidal gratings exhibit some characteristic differences. The lamellar grating emits radiation in sharp peaks, with an optimum electron energy of about 2 MeV. For the sinusoidal grating the emission is stronger in the forward direction and optimum electron energies are at about 10 MeV. Apparently, the use of high-energy electron beams is of no advantage in this spectral range. This may be different in the x-ray energy domain, where our model is not valid. When using relativistic electrons ($c_0/v_0 \approx 1$) photons of very short wavelength are emitted in forward directions $\eta \approx 90°$. For example, using a commercial optical grating of 1800 lines per millimeter, at $\eta = 80°$ the corresponding wavelength is $\lambda = 84$ Å. At such short wavelengths, however, the hypothesis of a perfect conducting surface fails and one has to use a more complete theoretical model including the conductivity $\sigma(\lambda)$. In addition, the small ratio $\lambda/D$ implies a very large number of diffracted orders. Under these circumstances the solution of the integral equations becomes awkward and an asymptotic theory for the diffraction of small wavelengths at large incident angles should be used. Due to these difficulties we have restricted our calculations to (i) wavelengths for which the conductivity of the surface can be considered as infinity, i.e., from infrared to visible light, (ii) gratings for which the ratio $\lambda/D$ is not too small, and (iii) emission angles that are not too close to the forward direction, typically $\eta < 45°$.

Figure 11 shows a comparison of SP spectra using a 5-MeV accelerator and different gratings. A set of gratings with different parameters could be used to taylor the SP radiation spectra to the experimental needs. By collimation of the SP radiation into a solid angle $\Delta\Omega = \cos(\eta)\Delta\eta\Delta\zeta$ one obtains radiation of bandwidth $\Delta\lambda/\lambda = \cos(\eta)[\beta^{-1} - \sin(\eta)]^{-1}\Delta\eta$ in first order. Using a 5-MeV electron beam and a lamellar grating, a peak photon flux of $5 \times 10^{13}$ s$^{-1}$ in a solid angle of 1 $\mu$sr can be obtained [cf. the maximum of curve ($a$) near $\lambda = 1$ mm in Fig. 11]. This photon flux would be quasimonochromatic with a bandwidth $\Delta\lambda/\lambda \approx 10^{-3}$. Continuous tuning of the peak intensity in the SP spectra is also possible by varying the electron energy. Figure 12 shows spectra calculated for a 1-mm lamellar grating at several electron energies between 5 and 8 MeV. The peak is shifted from 1.04 to 1.18 mm when the electron energy increases from 5 to 8 MeV.

For electron energies of 350 keV we obtain $h_{\text{int}} \approx \lambda/10$ at $\zeta = 0°$. This means that at very low electron energies very small beam sizes are needed in order to get a reasonable fraction of the electrons interacting effectively with the grating. Furthermore, careful alignment of the electron beam close and parallel to the grating surface is mandatory. At 10 MeV we find $h_{\text{int}} \approx 1.6\lambda$ and at 100 MeV $h_{\text{int}} \approx 16\lambda$, which means that for production of photons in the far infrared or millimeter range even electron beams with a diameter of the order of 1–10 mm would still be efficient. Indeed the entire beam would interact with the grating and even the positioning of the beam above the grating is not critical. In the far infrared aluminum gratings with periods $D \leq 1$ mm can be used taking advantage of (i) an electrical conductivity that can be considered as infinite in this spectral range and (ii) a very good thermal conductivity, which reduces the risk of possible damage caused by the beam. Such gratings can easily be produced.

From these technical considerations it appears that accelerators of moderate energy and relatively low cost could be used as strong sources of SP radiation in the long-wavelength range. The results of Doucas *et al.* [1] using a 3.6-MeV electron beam confirm this expectation.

### C. Extensions of the model

As mentioned above, the SP effect could also be used to produce radiation in the uv and soft-x-ray energy domain using high-energy electron beams. In this spectral range a finite electrical conductivity $\sigma(\lambda)$ has to be included in the boundary condition (2.9). Although this problem has been treated [30] for nonrelativistic velocities $v_0 \ll c_0$, to our knowledge there is at present no rigorous theory of SP radiation available including a finite conductivity of the grating surface.

In order to obtain short wavelengths of SP radiation, observation angles close to the forward direction $\eta \approx 90°$ have to be chosen. This implies a very large number of diffracted orders, which makes the solution of the integral equations difficult. In a recent publication Moran [31] presented a different approach adapting the Ter-Mikaelian [32] description of radiation produced when a relativistic electron passes a linear slit to the grating problem. In this approach, the radiation is expressed in a closed form, which is very convenient for designing SP experiments. It assumes, however, infinitely thin screens, an assumption which may be questionable for photon wavelengths around 100 Å.

In all our calculations we assumed an electron trajectory perpendicular to the grating rulings. Steering the electron beam at some angle to this direction but still parallel to the surface of the grating would allow to tune the SP spectra because the effective grating period seen by the electron is changed. Maystre and Petit [33] and van den Berg [16] have treated the general case of conical diffraction in spectroscopy, where the incident light does not fall on the grating perpendicularly to the rulings. In the SP approach [17] we have used in our calculations conical diffraction at finite observation angles $\zeta \neq 0°$ is already included. Therefore it should be possible to adapt these models to the case of SP radiation when the electron beam travels at an arbitrary angle relative to the grating rulings.

### D. Estimate of a SP free-electron-laser gain

In the preceding sections we have restricted the discussion to spontaneous SP radiation. The stimulated emis-

sion of SP radiation, problems related to the active coupling of the electron beam to the electromagnetic surface waves [8–11,34–36] and the presence of a strong guiding magnetic field [37,38] have not been taken into consideration. With some simplifying assumptions, however, we can estimate the stimulated emission gain from the calculated spontaneous emission power. Friedman *et al.* [39] have derived general relations between spontaneous and stimulated emission of radiation for several quasi-free-electron radiation effects. For an open resonator SP free-electron laser (FEL) they get for the gain at maximum gain detuning point [39]

$$g_{\max}=0.54\pi\frac{|n|\lambda^2L^2}{mc_0^3A_{\text{e.m.}}D\beta^3\gamma^3}\times(1+\beta^2\gamma^2\cos^2\eta\sin^2\zeta)\left[\frac{dP}{d\Omega}\right]_{\text{sp}}, \tag{5.3}$$

in which $m$ is the electron mass and $A_{\text{e.m.}}$ is the effective radiation beam cross section. We take the radiation beamwidth equal to the full width at half maximum of the electron beam in $y$ direction and the length of the radiation beam spot on the grating equal to the grating length, i.e., $A_{\text{e.m.}}=\sqrt{8\ln 2}\sigma_y L\cos\eta$. Friedman *et al.* [39] give an example based on experimental values [18] obtained using a 100-keV electron beam and a blazed grating with $D=556$ nm and $h/D\approx\frac{1}{3}$. In this experiment $5.8\times10^{-10}$ W/sr were observed in second order at $\eta=-16°$ and $\zeta=50°$, which gives a maximum gain $g_{\max}=5.6\times10^{-8}$. This rather low value is mainly due to (i) the relatively low beam current of 0.25 $\mu$A used in the experiment and (ii) the fact that the dimension of the beam in $z$ direction was rather large ($h_{\text{int}}/\sigma_z\approx3\times10^{-4}$). For comparison, we use Eq. (5.3) to calculate the maximum gain for some of the parameters used in the discussion of spontaneous SP radiation in the preceding sections. At 1 MeV and using a lamellar grating we find from Fig. 9(a) a gain of $g_{\max}\approx13\%$ at $\lambda=0.7$ mm ($h_{\text{int}}/\sigma_z\approx0.1$) and $g_{\max}\approx5.5\%$ at $\lambda=0.42$ mm ($h_{\text{int}}/\sigma_z\approx0.06$). At 2 MeV we get from Fig. 9(b) a value $g_{\max}\approx6\%$ at $\lambda=0.7$ mm ($h_{\text{int}}/\sigma_z\approx0.2$) and at 5 MeV we find from curve ($a$) of Fig. 11 a gain of $g_{\max}\approx1.7\%$ at $\lambda=1.03$ mm ($h_{\text{int}}/\sigma_z\approx0.6$). As emphasized above, we did not attempt to optimize the different parameters in order to find a maximum power of SP radiation. We also did not investigate the applicability of Eq. (5.3) to the experimental configurations for which these values were calculated. The main objective of these simple considerations is merely to illustrate that it might be worthwhile to consider in the design of a SP FEL such parameters as the grating profile, electron energy, and observation angles in order to choose optimum values for maximum spontaneous emission of SP radiation.

## VI. CONCLUSIONS

We have calculated SP radiation produced by relativistic electrons of 1–100 MeV in the frame of an electromagnetic theory. Some techniques to solve the grating problem have been discussed. In our calculations we used the integral method, which is of most general validity. For lamellar gratings and an observation angle $\zeta=0°$ we also used the modal expansion method and for shallow sinusoidal gratings the improved point-matching method, which both require less computational effort. Good agreement was found between the results of these specialized methods and the integral method. Special attention was given to the case of high-energy electrons with $v_0/c_0\approx1$. The results show that in the millimeter wavelength range reasonable intensities of SP radiation could be obtained using 1–10-MeV electrons. High-energy electrons are of no advantage in this spectral range. The models used in our calculations do not include a finite electrical conductivity $\sigma(\lambda)$. Also, due to numerical difficulties, these models are not applicable at forward angles. Therefore our conclusions do not apply for generation of SP radiation in the uv or x-ray energy range. The SP effect seems to be a good candidate for the construction of coherent, tunable radiation sources. By careful selection of the grating special characteristics of the radiation can be adapted to the experimental needs, e.g., tunability, broad spectral range of moderate intensity, or large intensity concentrated in a few peaks of narrow bandwidth. The use of oblique incidence of the electrons for convenient tuning of the SP radiation remains to be investigated. The emittance of the electron beam becomes a severe limitation for generation of SP radiation in the uv and soft-x-ray energy domain but is less crucial at longer wavelengths.

## ACKNOWLEDGMENTS

We wish to express our gratitude to L. Wartski for drawing our attention to this interesting subject and for valuable theoretical advise. One of us (O.H.) gratefully acknowledges the help of J. Hartong on several mathematical problems. We also thank P. M. van den Berg for an interesting discussion of his work on the SP effect.

[1] G. Doucas, J. H. Mulvey, M. Omori, J. Walsh, and M. F. Kimmit, Phys. Rev. Lett. **69**, 1761 (1992).
[2] I. Amato, Science **16**, 401 (1992).
[3] G. Dattoli and A. Renieri, Phys. World **6** (1), 25 (1993).
[4] I. M. Frank, Izv. Akad. Nauk SSSR Ser. Fiz. **6**, 3 (1942).
[5] S. J. Smith and E. M. Purcell, Phys. Rev. **92**, 1069 (1953).
[6] W. W. Salisbury, J. Opt. Soc. Am. **60**, 1279 (1970).
[7] K. Mizuno, S. Ono, and O. Shimoe, Nature **253**, 184 (1975).
[8] F. S. Rusin and G. D. Bogomolov, Proc. IEEE **57**, 720

(1969).
[9] J. M. Wachtel, J. Appl. Phys. **50**, 49 (1979).
[10] R. P. Leavitt, D. E. Wortman, and H. Dropkin, IEEE J. Quantum Electron. **QE-17**, 1333 (1981).
[11] R. P. Leavitt, D. E. Wortman, and H. Dropkin, IEEE J. Quantum Electron. **QE-17**, 1341 (1981).
[12] G. Toraldo di Francia, Nuovo Cimento **16**, 1065 (1961).
[13] G. V. Voskresenskii and B. M. Bolotovskii, Dokl. Akad. Nauk SSSR **156**, 770 (1964) [Sov. Phys. Dokl. **9**, 459 (1964)].
[14] J. P. Bachheimer, C. R. Acad. Sci. B **268**, 599 (1969).
[15] R. Petit and D. Maystre, Rev. Phys. Appl. **7**, 427 (1972).
[16] P. M. van den Berg, Appl. Sci. Res. **24**, 261 (1971).
[17] P. M. van den Berg, J. Opt. Soc. Am. **63**, 1588 (1973).
[18] A. Gover, P. Dvorkis, and U. Elisha, J. Opt. Soc. Am. B **1**, 723 (1984).
[19] J. P. Bachheimer, Phys. Rev. B **6**, 2985 (1972).
[20] *Electromagnetic Theory of Gratings,* edited by R. Petit (Springer-Verlag, Berlin, 1980).
[21] J. P. Bachheimer, Ph.D. thesis, Université Scientifique et Medicale Grenoble, 1971.
[22] R. Petit and R. M. Cadilhac, C. R. Acad. Sci. B **262**, 468 (1966).
[23] W. C. Meecham, J. Appl. Phys. **27**, 361 (1956).
[24] H. Ikuno and K. Yasuura, IEEE Trans. Antennas Propag. **AP-2**, 657 (1973).
[25] R. F. Millar, Radio Sci. **8**, 785 (1973).
[26] P. M. van den Berg, J. Opt. Soc. Am. **71**, 1224 (1981).
[27] P. M. van den Berg, J. Opt. Soc. Am. **64**, 325 (1974).
[28] L. N. Deryugin, Radio Eng. Electron. Phys. (USSR) **15**, 25 (1960).
[29] S. Jovicevic and S. Sesnic, J. Opt. Soc. Am. **62**, 865 (1972).
[30] J. C. McDaniel *et al.*, Appl. Opt. **28**, 4924 (1989).
[31] M. J. Moran, Phys. Rev. Lett. **69**, 2523 (1992).
[32] M. L. Ter-Mikaelian, *High-Energy Electromagnetic Processes in Condensed Media* (Wiley Interscience, New York, 1972), p. 382.
[33] D. Maystre and R. Petit, Opt. Commun. **4**, 97 (1971).
[34] J. E. Walsh *et al.*, IEEE J. Quantum Electron. **QE-21**, 920 (1985).
[35] K. Yasumoto, T. Tanaka, and T. Aramaki, IEEE Trans. Plasma Sci. **18**, 699 (1990).
[36] B. Hafizi, P. Sprangle, and P. Serafim, Phys. Rev. A **45**, 8846 (1992).
[37] L. Schächter, J. Opt. Soc. Am. B **7**, 873 (1990).
[38] L. Schächter, J. Appl. Phys. **67**, 3582 (1990).
[39] A. Friedman *et al.*, Rev. Mod. Phys. **60**, 471 (1988).